Journal of Theoretical Biology 567 (2023) 111496

Contents lists available at ScienceDirect

Journal of Theoretical Biology

journal homepage: www.elsevier.com/locate/yjtbi

Critical observation of WHO recommended multidrug therapy on the disease leprosy through mathematical study

Salil Ghosh [a], Shubhankar Saha [b], Priti Kumar Roy [a,*]

[a] Centre for Mathematical Biology and Ecology, Department of Mathematics, Jadavpur University, Kolkata - 700032, India
[b] Department of Mathematics, Sir Gurudas Mahavidyalaya, Kolkata - 700067, India

ARTICLE INFO

Keywords:
Leprosy mathematical modelling
Multidrug therapy
Drug efficacy
Hopf-bifurcation
Infection of Schwann cells

ABSTRACT

Leprosy is a skin disease and it is characterized by a disorder of the peripheral nervous system which occurs due to the infection of Schwann cells. In this research article, we have formulated a four-dimensional ODE-based mathematical model which consists of the densities of healthy Schwann cells, infected Schwann cells, *M. leprae* bacteria, and the concentration of multidrug therapy (MDT). This work primarily aims on exploring the dynamical changes and interrelations of the system cell populations during the disease progression. Also, evaluating a critical value of the drug efficacy rate of MDT remains our key focus in this article so that a safe drug dose regimen for leprosy can be framed more effectively and realistically. We have examined the stability scenario of different equilibria and the occurrence of Hopf-bifurcation for the densities of our system cell populations with respect to the drug efficacy rate of MDT to gain insight on the precise impact of the efficiency rate on both the infected Schwann cell and the bacterial populations. Also, a necessary transversality condition for the occurrence of the bifurcation has been established. Our analytical and numerical investigations in this research work precisely explores that the process of demyelination, nerve regeneration, and infection of the healthy Schwann cells are the three most crucial factors in the leprosy pathogenesis and to control the *M. leprae*-induced infection of Schwann cells successfully, a more flexible version of MDT regime with efficacy rate varying in the range $\eta \in (0.025, 0.059)$ for $100 - 120$ days in PB cases and 300 days in MB cases obtained in this research article should be applied. All of our analytical outcomes have been verified through numerical simulations and compared with some existing clinical findings.

1. Introduction

Among all non-traumatic peripheral neuropathies worldwide, leprosy is the most complicated and poorly understood disease which is caused by a bacterium called *Mycobacterium leprae* (*M. leprae*). Currently, more than three million people are suffering from the severe neurological disabilities caused due to leprosy (Ng et al., 2000). It is very concerning to the epidemiologists that the new case detection rate and disease prevalence of leprosy remains extremely high especially in the developing countries and it is expected that leprosy is not going to disappear anytime soon in spite of the introduction of MDT (multidrug therapy) (Lockwood and Suneetha, 2005; Meima et al., 2004). Also, the chronic mycobacterial infection and the associated immunologic events during the disease progression have often severe long-term physical, social, and psychological impacts (Scollard et al., 2006). In depth analytical investigation needs to be performed to unfold the complexities of the disease and strict preventive measures should be taken to eradicate leprosy from mankind. The primary entry route of *M. leprae* into the human body is the upper respiratory tract and transmission occurs through nasal mucosa and droplets from infected persons. Skin sores, lump, loss of feeling in hands and legs are some basic symptoms of leprosy which is caused due to the peripheral nerve damage during the course of infection. Also Leprosy may lead to blindness and harm the thin linings within the nose (White and Franco-Paredes, 2015). *M. leprae* exhibits specific molecular attraction to the Schwann cells of the axons of the peripheral nervous system via some receptors namely laminin-2 and alpha-dystroglycan complex (Rambukkana, 2001). The dedifferentiation of Schwann cells into immature cells caused by *M. leprae* provides not only a natural host but a safe and ideal habitat for the bacteria to proliferate and eventually, it leads to generating stem-cell like cells which spread the infection using its cellular plasticity property (Masaki et al., 2013; Rambukkana, 2010). The host immune responses to *M. leprae* produce natural clinical manifestations which subsequently leads to acute peripheral nerve damage (Wilder-Smith and Van Brakel, 2008). Specific *T* cells realize

* Corresponding author.
E-mail address: pritiju@gmail.com (P.K. Roy).

https://doi.org/10.1016/j.jtbi.2023.111496
Received 15 September 2022; Received in revised form 3 April 2023; Accepted 11 April 2023
Available online 18 April 2023

the presence of intracellular *M. leprae* after some time and it induces severe chronic inflammatory immunological reactions. This process results in swelling within the perineurium and further nerve damage with axonal death (Britton, 1998).

Before 1982, the only available treatment for leprosy was dapsone monotherapy but drug resistance to dapsone was observed in a large number of patients suffering from leprosy. So, multidrug therapy (MDT) was implemented according to the recommendation of World Health Organization in 1982 (Walker and Lockwood, 2006). The components of MDT are dapsone, rifampicin and clofazimine. Among these, dapsone has a bacteriostatic effect and rifampicin has a bactericidal effect on *M. leprae* while clofazimine mainly acts as an anti-inflammatory drug (Fischer, 2017). High concentrations of pro-inflammatory cytokines are observed in skin lesions of some patients treated with steroids even after 6 months of treatment. In a recent study with different amount of initial doses and different drug therapeutic schedules for leprosy, it is suggested that the rate at which infected nerve regenerates is nearly about 60% to 70% and the recovery rate relatively slow for patients with chronic and recurrent nerve impairment (WJ, 2004). Also, the results from clinical trials conducted in 2012 indicates that bacteriological index (BI) are observed to be decreased significantly over time in patients taking U-MDT compared to the regular MDT therapy but the relapse rates for U-MDT regimen are still a matter of concern for the clinical scientists (Kroger et al., 2008; Penna et al., 2014).

There are some previous works on various infectious diseases such as HIV which dealt with the infection of healthy cells, stable production of virus (Ikeda et al., 2003) and the key relationships in between the disease prevalence or infection rate, drug-efficacy and dosing regimen of the prescribed combined or single drug therapy into a human body (Smith and Wahl, 2005; Saha et al., 2018; Cao et al., 2019). On the disease leprosy, some mathematicians have established human population based compartmental mathematical models where investigation are performed on the transmission of infections and prevalence of leprosy into different community, age-group of people of different regions. Recently, Ghosh et al. (2021) developed and investigated a cell-dynamical mathematical model on leprosy where basic infection mechanism of healthy Schwann cells and intracellular proliferation of *M. leprae* were focused primarily for finding a safe and cost-effective optimal control strategy. But, no cell dynamical mathematical model has been constituted yet which incorporates the efficacy of MDT drug therapy and its interplay with the bacterial growth, progression of infection and most importantly, the mechanism of healthy cells being infected again due to fading effect of MDT, nerve impairment and the demyelination process in leprosy. As far as finding a perfect drug dose regimen for both paucibacillary (PB) and multibacillary (MB) leprosy is our foremost goal, in depth investigation of the drug efficacy of the existing MDT therapy and its correlations with various pathogenetic components of leprosy must be given major importance to eradicate the disease permanently from mankind.

In this research article, we have proposed a four dimensional nonlinear ODE based mathematical model to investigate the cell-dynamical interactions of healthy Schwann cells, infected Schwann cells, *M. leprae* bacteria and their internal relations with the drug efficiency of MDT used to treat leprosy. Boundedness and positive invariance for our system have been studied in this paper by finding an invariant region while different equilibria of the system are discussed extensively to achieve significant conditions that present an overall description of the stability situation of our system. We have also provided a detailed analysis of the appearance of Hopf-bifurcation for our system and as a consequence of this, a critical value of the bifurcation parameter has been evaluated. Throughout the article, our main objective remains to explore the variety of neurological manifestations and pathophysiology of nerve damage in leprosy which enables us to predict the perfect drug dose regimen for the treatment of the nerve-function impairment. Also, we have studied the precise effects of multidrug therapy on the system cell populations. In particular, we have investigated how MDT treatment regulates the recovery of infected cells and the infection process of the healthy cells due to the waning effect of MDT and established that it is actually the drug efficacy rate of MDT which plays a significant dominant role in the pathogenesis and treatment of leprosy. All the analytical outcomes obtained in this article have been verified through numerical simulations. Based on the clinical, histological and immunological differences, Ridley–Jopling classification of leprosy provides a complete spectrum of five main categories i.e. TT, BT, BB, BL and LL (Ridley and Jopling, 1966). Ridley's bacterial index (BI) with BI $\geq$ 2 (skin lesions $>$ 5) forms the multibacillary group (MB) consisting of BB, BL and LL patients while BT and TT leprosy patients are categorized as paucibacillary group (PB) (Parkash, 2009). In real life scenario, clinical correlations of our research findings with U-MDT regimen, Ridley–Jopling classification and WHO recommended guidelines for leprosy are discussed in detail.

This manuscript is organized as follows. In Section 2, the mathematical model formulation along with the suitable assumptions has been described. Some basic model properties such as the existence conditions and stability criteria of different equilibria for our formulated model have been derived in Section 3. Moreover, Section 4 is solely dedicated for the investigation of the appearance of Hopf-bifurcation for our system. In Section 5, we have illustrated numerical simulations of our system in different aspects to validate and justify the findings achieved in the previous sections. Finally, in Section 6, we have discussed the novelty of our model, obtained results, conclusions and predictions about the futuristic works on leprosy.

2. Formulation of the mathematical model

Following assumptions are made for the formulation of desired mathematical model:

- The concentrations of healthy Schwann cells, infected Schwann cells, *M. leprae* bacteria and MDT drug therapy are represented by $S_h(t)$, $S_i(t)$, $B(t)$ and $X(t)$ respectively, at any time t.
- Π denotes the constant production rate of healthy Schwann cells from neural crest cells into human body. β is the effective contact rate between the healthy Schwann cells and the bacteria. α be the rate at which infected cells become recovered due to the effect of MDT. The rate at which healthy Schwann cells are getting infected again as a result of waning effect of MDT is indicated by λ.
- The parameters, r and K describe the intrinsic growth rate and carrying capacity of M. leprae bacteria as presented in a logistic manner.
- The level of treatment i.e. the concentration of MDT is proportional to the number of infected Schwann cells and it is represented by the term, $e\eta S_i$, where e denotes the proportionality constant and η denotes the efficacy rate of MDT. Moreover, θ reflects the natural drug washout rate through various physiological processes into a human body.
- d, d_i and d_b signify the natural death rate or mortality rate healthy Schwann cells, infected Schwann cells and the rate at which *M. leprae* bacteria is killed by MDT, respectively.
- The effective drug-treatments is directed by the increasing function, $f(X)$ with $f(0) = 0$ and $\sup f(X) = 1$. It is considered that the effectiveness of drug is fading for which the healthy Schwann cells are becoming infected again. Therefore, $g(X)$ is chosen as a decreasing function of X with $g(0) = 1$ and $\inf g(X) = 0$.

Based on the above assumptions, we have the following mathematical model which depict the various interactions between the compartments:

$$\frac{dS_h}{dt} = \Pi - \beta S_h B + \alpha f(X) S_i - \lambda g(X) S_h - d S_h,$$
$$\frac{dS_i}{dt} = \beta S_h B - \alpha f(X) S_i + \lambda g(X) S_h - d_i S_i,$$

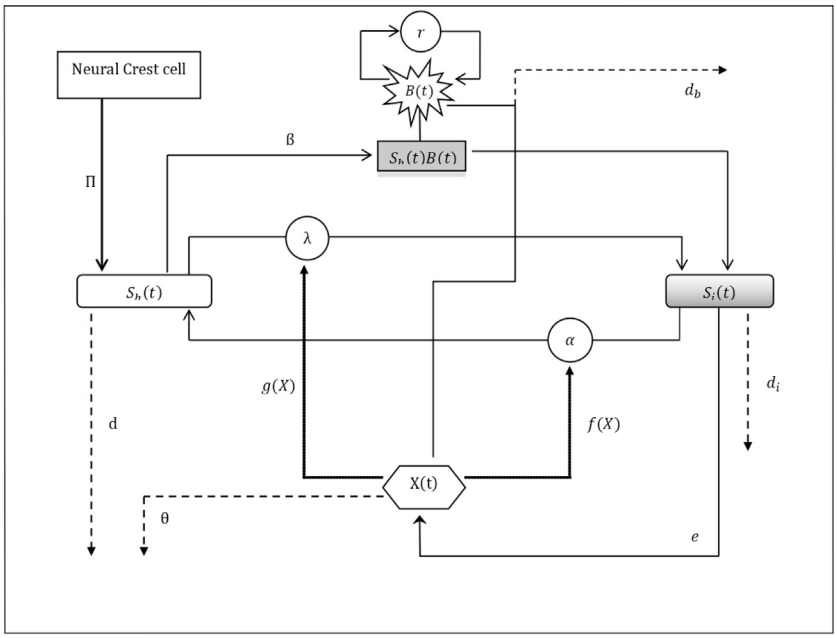

Fig. 1. Schematic diagram of the interactions of the cell populations for system (1).

$$\begin{aligned}\frac{dB}{dt} &= rB\left(1-\frac{B}{K}\right) - d_b X B,\\ \frac{dX}{dt} &= e\eta S_i - \theta X\end{aligned} \tag{1}$$

with initial values $S_h(0) = S_{h0} > 0$, $S_i(0) = S_{i0} > 0$ and $B(0) = B_0 > 0$ and $X(0) = X_0 > 0$ at $t = 0$ (see Fig. 1).

3. Model properties

3.1. Non-negative invariance and boundedness

In this subsection, we discuss the non-negativity of the solutions and boundedness of our proposed mathematical model to prove that the system (1) is biologically well-posed and plausible. We now present the following theorem which ensures the non-negativity of the solutions of system (1).

Theorem 3.1. *All the solutions of the system (1) along with the initial conditions are non-negative for all $t > 0$.*

Proof. To prove the theorem, let us first assume that $y_1(t) = S_h(t)$, $y_2(t) = S_i(t)$, $y_3(t) = B(t)$ and $y_4(t) = X(t)$. Now, we can rewrite system (1) in the following form:

$$\frac{dY}{dt} = \Gamma(Y), \quad \Gamma = (\Gamma_1, \Gamma_2, \Gamma_3, \Gamma_4)^\top, \quad Y = (y_1, y_2, y_3, y_4)^\top \tag{2}$$

where $^\top$ denotes the transpose and Γ_i's denote the right hand sides of system (1).

Now, for system (2), it is easy to check that

$$\Gamma_i(Y)\big|_{y_i=0,\ Y\in\mathbb{R}^4_+} \geq 0. \tag{3}$$

Indeed, we can see that the following relations hold.

$$\begin{aligned}&\Gamma_1(0, y_2, y_3, y_4) = \Pi + \alpha f(y_4) y_2 \geq 0, \quad \text{whenever} \quad y_2 \geq 0, y_3 \geq 0, y_4 \geq 0,\\ &\Gamma_2(y_1, 0, y_3, y_4) = \beta y_1 y_3 + \lambda g(y_4) y_1 \geq 0, \quad \text{whenever} \quad y_1 \geq 0, y_3 \geq 0, y_4 \geq 0,\\ &\Gamma_3(y_1, y_2, 0, y_4) = 0, \quad \text{whenever} \quad y_1 \geq 0, y_2 \geq 0, y_4 \geq 0,\\ &\Gamma_4(y_1, y_2, y_3, 0) = e\eta y_2 \geq 0, \quad \text{whenever} \quad y_1 \geq 0, y_3 \geq 0, y_4 \geq 0.\end{aligned}$$

Thus, using the result in Krasnosel'skii (1968), we can say that the conditions denoted by (3) clearly ensures the non-negativity of the solutions $y_1(t)$, $y_2(t)$, $y_3(t)$ and $y_4(t)$ of system (1) under the given initial conditions. It means that all the solutions of the system (1) exists in the region $\mathbb{R}^4_+$ and the solutions remain non-negative for all $t > 0$. This also implies that the non-negative octant $\mathbb{R}^4_+$ becomes an invariant region for system (1). □

It is also very essential to prove that all the model cell populations of system (1) are bounded for all time $t > 0$. This justifies that the system (1) is well-posed and realistic. The next theorem demonstrates the boundedness of the solutions of system (1).

Theorem 3.2. *All the non-negative solutions of system (1) enter the domain denoted by $\mathcal{D} \subset \mathbb{R}^4_+$ and are ultimately bounded for all possible time $t > 0$ where the region $\mathcal{B}$ is defined as:*

$$\mathcal{B} = \left\{(S_h, S_i, B, X) \in \mathbb{R}^4_+ : 0 \leq S_h + S_i \leq \mathcal{D}_1, 0 \leq B \leq \mathcal{D}_2, 0 \leq X \leq \mathcal{D}_3\right\} \tag{4}$$

where $\mathcal{D}_i$'s for $i = 1, 2, 3$ are given as:

$$\mathcal{D}_1 = \frac{\Pi}{d}, \quad \mathcal{D}_2 = max\ \{K, B(0)\} \quad and \quad \mathcal{D}_3 = \frac{e\eta\Pi}{\theta d}.$$

Proof. First, let us consider the first two equations of system (1). Adding these two equations, we get

$$\frac{d(S_h + S_i)(t)}{dt} = \Pi - (d + d_i)(S_h + S_i)(t)$$

which implies

$$\frac{dU(t)}{dt} \leq \Pi - dU(t) = d\mathcal{D}_1 - dU(t), \tag{5}$$

where $U(t) = (S_h + S_i)(t)$. Now, using the well-known comparison principle (Birkhoff and Rota, 1978) to (5), we achieve the following inequality:

$$0 < U(t) < \mathcal{D}_1(1 - e^{-dt}) + U(0)e^{-dt} \quad \text{for} \quad t > 0. \tag{6}$$

This implies that $U(t) \leq \mathcal{D}_1$ if $U(0) \leq \mathcal{D}_1$.

Now, we consider the third equation of system (1). Using Theorem 3.1, we can write the following inequality:

$$\frac{dB(t)}{dt} \leq rB(t)(1 - \frac{B(t)}{K}). \tag{7}$$

Integrating this inequality with the corresponding initial condition i.e. $B(0) > 0$, we get

$$0 \le B(t) \le \frac{K B(0)}{B(0)(1-e^{-rt}) + K e^{-rt}} \le \mathcal{D}_2 \tag{8}$$

where $\mathcal{D}_2 = max\ \{K, B(0)\}$.

Again, using the result $0 \le S_i \le \frac{\Pi}{d}$ and repeating the similar argument, we also obtain the following:

$$0 < X(t) < \mathcal{D}_3(1-e^{-\theta t}) + X(0)e^{-\theta t} \quad \text{for} \quad t > 0 \tag{9}$$

which implies that $X(t) \le \mathcal{D}_3$ if $X(0) \le \mathcal{D}_3$.

Hence, all the solutions (S_h, S_i, B, X) of system (1) which start in the region $\mathcal{B}$, remain within it for all $t > 0$. This evidently makes $\mathcal{B}$ an invariant region for system (1). Also, the region $\mathcal{B}$ is bounded and this implies that all the mentioned solutions of the system (1) are ultimately bounded.

Here, it is important to note that all such solutions of system (1) with the non-negative initial conditions finally arrive into $\mathcal{B}$ and stay in it. This property is justified by the definition of the region $\mathcal{B}$ and the following relationships:

$$\begin{aligned} &\frac{dS_h}{dt}(t)\Big|_{\partial\mathcal{B}} < 0, \qquad \frac{dS_i}{dt}(t)\Big|_{\partial\mathcal{B}} < 0, \\ &\frac{dB}{dt}(t)\Big|_{\partial\mathcal{B}} < 0, \qquad \frac{dX}{dt}(t)\Big|_{\partial\mathcal{B}} < 0, \end{aligned} \tag{10}$$

which are actually carried out at the points of the boundary $\partial\mathcal{B}$ of $\mathcal{B}$. Also, note that, the relationships in (10) hold outside the region $\mathcal{B}$ which completely ensures the boundedness of all solutions (S_h, S_i, B, X) of system (1) with the above mentioned non-negative initial conditions. □

3.2. Equilibrium points and their existence

In this section, some basic properties such as existence and stability of equilibria for system (1) are illustrated.

The equilibrium points are obtained by equating the right-hand side of each equation in (1) to zero and it is found that system (1) has two non-negative equilibria, namely

- the trivial disease-free equilibria $E_0 = \left(\frac{\Pi}{d}, 0, 0, 0\right)$, which always exists,
- for the endemic equilibrium $E^*(S_h^*, S_i^*, B^*, X^*) \neq 0$ to exist, its coordinates must satisfy the following conditions: $S_h^* > 0$, $S_i^* > 0$, $B^* > 0$ and $X^* > 0$ where

$$S_h^* = \frac{r[\alpha f(X^*) + d_i]\theta X^*}{e\eta[\beta K(r - d_b X^*) + r\lambda g(X^*)]}, \quad S_i^* = \frac{\theta X^*}{e\eta},$$
$$B^* = \frac{K}{r}(r - d_b X^*) \quad \text{and} \quad X^* = \frac{r}{d_b}(1 - \frac{B^*}{K}).$$

Here, using Theorem 3.2 i.e the fact that the bacterial concentration $B(t)$ cannot exceed the carrying capacity K of the *M. leprae* bacterial population, it follows that $X^* = \frac{r}{d_b}(1 - \frac{B^*}{K}) > 0$. Also, this implies that $S_i^* = \frac{\theta X^*}{e\eta} > 0$ as $X^* > 0$.

Now, considering the formulas of S_h^* and B^*, we can see that both $S_h^* > 0$ and $B^* > 0$ provided the condition $r > d_b X^*$ holds. This ensures the existence of positive endemic equilibrium E^* of system (1). We now summarize the previous discussions by constructing the following lemma.

Lemma 3.1. *The positive endemic equilibrium E^* of system (1) exists if $r > d_b X^*$ is satisfied.*

Remark 3.1. The sufficient condition for the existence of the endemic equilibrium E^* is that whenever the ratio of intrinsic growth rate and the rate at which M. leprae bacteria is killed by the drug therapy, exceeds X^*. Biologically, this is well supported as it means that the growth rate (r) of the bacterial population and the killing rate (d_b) of the bacteria by MDT plays a crucial role in this scenario and if the ratio becomes relatively higher than endemic state MDT concentration X^*, the infected steady state becomes feasible i.e begins to exist.

3.3. Stability analysis

In this section, at first, we deduce the basic reproduction number R_0 and discuss the local asymptotic stability of the disease-free equilibrium E_0.

Biologically, we can say that R_0 is the average number of new secondary infections in a completely susceptible Schwann cell population. To evaluate R_0, we choose the next-generation matrix method (Heffernan et al., 2005). We consider only the infected compartments ($S_i(t)$, $B(t)$ and $X(t)$) of system (1) i.e. to be precise, the second, third and fourth equations of system (1). Now, let us define the three dimensional matrices $\mathcal{F}$ and $\mathcal{V}$ as the matrices describing the new infection terms and the remaining transfer terms evaluated at the disease-free equilibrium $E_0 = \left(\frac{\Pi}{d}, 0, 0, 0\right)$, respectively. The linearization of the second, third and fourth equations of system (1) at the disease-free state E_0 can be rewritten in the following form:

$$\frac{dW}{dt} = (\mathcal{F} - \mathcal{V})W$$

where $W = (S_i, B, X)^\top$ and the matrices $\mathcal{F}$ and $\mathcal{V}$ are given as:

$$\mathcal{F} = \begin{pmatrix} 0 & \frac{\beta\Pi}{d} & \frac{\lambda q\Pi}{d} \\ 0 & 0 & 0 \\ e\eta & 0 & 0 \end{pmatrix} \quad \text{and} \quad \mathcal{V} = \begin{pmatrix} d_i & 0 & 0 \\ 0 & -r & 0 \\ 0 & 0 & \theta \end{pmatrix}. \tag{11}$$

Using the spectral radius of the next-generation matrix a threshold criterion i.e. the basic reproduction number R_0 can be determined which is actually the largest eigenvalue (ρ) of the matrix $\mathcal{F}\mathcal{V}^{-1}$. Hence,

$$R_0 = \rho(\mathcal{F}\mathcal{V}^{-1}) = \max_{|\kappa|} \det(\kappa I - \mathcal{F}\mathcal{V}^{-1})$$

where I is the identity matrix of order 3 and

$$\mathcal{F}\mathcal{V}^{-1} = \begin{pmatrix} 0 & -\frac{\beta\Pi}{dr} & \frac{\lambda q\Pi}{d\theta} \\ 0 & 0 & 0 \\ \frac{e\eta}{d_i} & 0 & 0 \end{pmatrix}. \tag{12}$$

So, finally we have

$$R_0 = \sqrt{\frac{\lambda\Pi q e\eta}{d d_i \theta}}. \tag{13}$$

Now, the discussion of local stability of disease-free equilibrium E_0 with respect to the basic reproduction number R_0 can be summarized in the following theorem.

Theorem 3.3. *The system is stable at E_0 if $R_0 < 1$ and becomes unstable for $R_0 > 1$. Consequently, a transcritical bifurcation occurs at the critical value $R_0 = 1$.*

At the endemic equilibrium $E^* = (S_h^*, S_i^*, B^*, X^*)$, the Jacobian matrix of system (1) takes the following form:

$$\mathcal{J}(E^*) = \begin{pmatrix} M_{11}^* & M_{12}^* & -M_{13}^* & -M_{14}^* \\ M_{21}^* & M_{22}^* & M_{13}^* & M_{14}^* \\ 0 & 0 & M_{33}^* & M_{34}^* \\ 0 & M_{42}^* & 0 & M_{44}^* \end{pmatrix}.$$

where $M_{11}^* = -(\beta B^* + \lambda g(X^*) + d) = -(M_{21}^* + d)$, $M_{12}^* = \alpha f(X^*)$, $M_{13}^* = \beta S_h^*$, $M_{14}^* = -\alpha f'(X^*)S_i^* + \lambda g'(X^*)S_h^*$, $M_{21}^* = \beta B^* + \lambda g(X^*)$, $M_{22}^* = -\alpha f(X^*) - d_i$, $M_{33}^* = r - \frac{2rB^*}{K} - d_b X^*$, $M_{34}^* = -d_b B^*$, $M_{42}^* = e\eta$, $M_{44}^* = -\theta$. Expanding $\det(\mathcal{J} - \upsilon I) = 0$, we get the characteristic equation of system (1) at the endemic equilibrium point E^* as follows:

$$Y(\upsilon) = \upsilon^4 + \psi_1\upsilon^3 + \psi_2\upsilon^2 + \psi_3\upsilon + \psi_4 = 0 \tag{14}$$

where

$$\begin{aligned}
\psi_1 &= -(M_{11}^* + M_{22}^* + M_{33}^* + M_{44}^*),\\
\psi_2 &= M_{33}^* M_{44}^* + M_{33}^*(M_{11}^* + M_{22}^*) + M_{44}^*(M_{11}^* + M_{22}^*)\\
&\quad + M_{11}^* M_{22}^* - M_{42}^* M_{14}^* - M_{21}^* M_{12}^*,\\
\psi_3 &= M_{42}^* M_{14}^*(M_{11}^* + M_{21}^* + M_{33}^*) - M_{33}^* M_{44}^*(M_{11}^* + M_{22}^*)\\
&\quad - M_{33}^*(M_{11}^* M_{22}^* - M_{21}^* M_{12}^*)\\
&\quad - M_{44}^*(M_{11}^* M_{22}^* - M_{21}^* M_{12}^*) - M_{13}^* M_{34}^* M_{42}^*,\\
\psi_4 &= M_{13}^* M_{34}^* M_{42}^*(M_{11}^* + M_{21}^*) + M_{33}^* M_{44}^*(M_{11}^* M_{22}^* - M_{21}^* M_{12}^*)\\
&\quad - M_{14}^* M_{33}^* M_{42}^*(M_{11}^* + M_{21}^*).
\end{aligned}$$

The characteristic equation $Y(\upsilon) = \upsilon^4 + \psi_1\upsilon^3 + \psi_2\upsilon^2 + \psi_3\upsilon + \psi_4 = 0$ denoted by Eq. (14) will play the dominant role in determining the local asymptotic stability of E^* for system (1). Hence, using Routh–Hurwitz criterion for system (1), we can obtain the following theorem:

Theorem 3.4. *At the endemic equilibrium point E^*, all the roots of the characteristic polynomial of system (1) will be negative real or possess negative real parts i.e. system (1) will be locally asymptotically stable at E^* if the following four conditions hold true:*

$$\psi_1 > 0, \quad \psi_4 > 0, \quad \psi_1\psi_2 > \psi_3 \quad \text{and} \quad \psi_1\psi_2\psi_3 - \psi_3^2 - \psi_1^2\psi_4. \tag{15}$$

In view of the above discussion, we can also present the following result.

Proposition 3.1. *The endemic equilibrium point E^* is stable if the condition $R_0 > 1$ is satisfied.*

4. Hopf-bifurcation analysis of the system

A system exhibits Hopf-bifurcation at the endemic steady state if the characteristic equation of the system at that state possesses a pair of purely imaginary eigenvalues and all the other eigenvalues are negative real or with negative real parts. We now study the local Hopf-bifurcation at the endemic equilibrium E^*. Here, for E^*, we consider $\zeta(= (\Pi, \beta, \alpha, \lambda, d, d_i, r, K, d_b, e, \eta, \theta)) \in \mathbb{R}$ is the generic bifurcation parameter of the system.

Let, $\Phi : (0, \infty) \longrightarrow \mathbb{R}$ be a continuously differentiable function of ζ defined as

$$\Phi(\zeta) = \psi_1(\zeta)\psi_2(\zeta)\psi_3(\zeta) - \psi_3^2(\zeta) - \psi_4(\zeta)\psi_1^2(\zeta). \tag{16}$$

For the hopf-bifurcation to occur, there exists a $\zeta^* \in (0, \infty)$ in the spectrum $\psi(\zeta) = \{\upsilon : Y(\upsilon) = 0\}$ of the characteristic Eq. (14), at which a pair of complex eigenvalues $\upsilon(\zeta^*)$ and $\bar{\upsilon}(\zeta^*) \in \psi(\zeta)$ satisfy the following two conditions:

$$\mathfrak{Re}[\upsilon(\zeta^*)] = 0, \quad \mathfrak{Im}[\upsilon(\zeta^*)] = \omega_0 > 0.$$

In addition, the following transversality condition also must have to be satisfied :

$$\left.\frac{d\mathfrak{Re}(\upsilon_j(\zeta))}{d\zeta}\right|_{\zeta=\zeta^*} \neq 0 \quad \text{for} \quad j = 1, 2. \tag{17}$$

Theorem 4.1. *The endemic equilibrium E^* of system (1) undergoes Hopf-bifurcation at $\zeta = \zeta^* \in (0, \infty)$ if and only if*

$$\psi_2(\zeta^*) > 0, \quad \psi_3(\zeta^*) > 0, \quad \psi_4(\zeta^*) > 0, \quad \psi_1(\zeta^*)\psi_2(\zeta^*) - \psi_3(\zeta^*) > 0, \tag{18}$$

$$\Phi(\zeta^*) = 0 \text{ and } \psi_1^3\psi_2'\psi_3(\psi_1 - 3\psi_3) - (\psi_2\psi_1^2 - 2\psi_3^2)(\psi_3'\psi_1^2 - \psi_1'\psi_3^2) \neq 0. \tag{19}$$

In addition, at $\zeta = \zeta^*$, the characteristic equation contains a pair of purely imaginary eigenvalues and the other two eigenvalues will be negative real or having negative real parts where differentiation with respect to ζ is denoted by primes.

Proof. From the condition, $\Phi(\zeta^*) = 0$, the characteristic Eq. (14) can be rewritten in the form

$$(\upsilon^2 + \frac{\psi_3}{\psi_1})(\upsilon^3 + \psi_1\upsilon + \frac{\psi_1\psi_4}{\psi_3}) = 0. \tag{20}$$

We now denote the four roots of Eq. (20) in the complex domain by υ_i for $i = 1, 2, 3, 4$ and let, the pair of imaginary roots at $\zeta = \zeta^*$ being $\upsilon_1 = \bar{\upsilon}_2$. Hence, we get that

$$\begin{cases} \upsilon_3 + \upsilon_4 = -\psi_1, \quad \omega_0^2 + \upsilon_3 + \upsilon_4 = \psi_2, \\ \omega_0^2(\upsilon_3 + \upsilon_4) = -\psi_3, \quad \omega_0^2\upsilon_3\upsilon_4 = \psi_4 \end{cases}$$

where $\omega_0 = \mathfrak{Im}\upsilon_1\zeta^*$. Considering this set of equations, we can see that $\omega_0 = \sqrt{\frac{\psi_3}{\psi_1}}$ and if ψ_3, ψ_4 are chosen as complex conjugates then we have that $2\mathfrak{Re}\upsilon_3 = -\psi_1$. From the characteristic Eq. (14), it follows that $\upsilon_3 < 0$, $\upsilon_4 < 0$ if υ_3, υ_4 are real roots. Now, to verify the transversality conditions, we substitute $\upsilon_j(\zeta) = \sigma_1(\zeta) \pm i\sigma_2(\zeta)$ in Eq. (14) and differentiating, it follows that

$$\begin{cases} K(\zeta)\sigma_1'(\zeta) - L(\zeta)\sigma_2'(\zeta) + M(\zeta) = 0, \\ L(\zeta)\sigma_1'(\zeta) + K(\zeta)\sigma_2'(\zeta) + N(\zeta) = 0, \end{cases} \tag{21}$$

where the values of $K(\zeta)$, $L(\zeta)$, $M(\zeta)$ and $N(\zeta)$ are given as

$$\begin{aligned}
K(\zeta) &= 4\sigma_1^3 - 12\sigma_1\sigma_2 + 3\psi_1(\sigma_1^2 - \sigma_2^2) + 2\psi_2\sigma_1 + \psi_3,\\
L(\zeta) &= 12\sigma_1^2\sigma_2 + 6\psi_1\sigma_1\sigma_2 - 4\sigma_1^3 + 2\psi_2\sigma_1,\\
M(\zeta) &= \psi_1\sigma_1^3 - 3\psi_1'\sigma_1\sigma_2^2 + \psi_2'(\sigma_1^2 - \sigma_2^2) + \psi_3'\sigma_1,\\
N(\zeta) &= 3\psi_1'\sigma_1^2\sigma_2 - \psi_1'\sigma_2^3 + 2\psi_2'\sigma_1\sigma_2 + \psi_3'\sigma_1.
\end{aligned}$$

Now, solving (21) for $\sigma_1'(\zeta)$, we get that

$$\begin{aligned}
\left.\frac{d\mathfrak{Re}(\upsilon_j(\zeta))}{d\zeta}\right|_{\zeta=\zeta^*} &= \sigma_1'(\zeta)\Big|_{\zeta=\zeta^*}\\
&= -\frac{[L(\zeta^*)N(\zeta^*) + K(\zeta^*)M(\zeta^*)]}{K^2(\zeta^*) + L^2(\zeta^*)}\\
&= \frac{\psi_1^3\psi_2'\psi_3(\psi_1 - 3\psi_3) - 2(\psi_2\psi_1^2 - 2\psi_3^2)(\psi_3'\psi_1^2 - \psi_1'\psi_3^2)}{\psi_1^4(\psi_1 - 3\psi_3)^2 + 4(\psi_2\psi_1^2 - 2\psi_3^2)^2}.
\end{aligned}$$

From this result, we can see that $\psi_1^4(\psi_1 - 3\psi_3)^2 + 4(\psi_2\psi_1^2 - 2\psi_3^2)^2 > 0$ always. Hence,

$$\left.\frac{d\mathfrak{Re}(\upsilon_j(\zeta))}{d\zeta}\right|_{\zeta=\zeta^*} \neq 0$$

holds if

$$\psi_1^3\psi_2'\psi_3(\psi_1 - 3\psi_3) - 2(\psi_2\psi_1^2 - 2\psi_3^2)(\psi_3'\psi_1^2 - \psi_1'\psi_3^2) \neq 0.$$

Thus, Hopf-bifurcation occurs for the critical value $\zeta = \zeta^*$ at a neighbourhood of the endemic equilibrium E^* of system (1). □

Remark 4.1. Hopf-bifurcating periodic solutions appear for our system cell populations in the neighbourhood of E^*. This indicates that the system (1) undergoes stability switches as an effect of administering MDT drug concentrations into the human body. The impact of λ as well as the infection rate β is notable here while the drug efficacy rate of MDT η contributes most significantly to this behaviour of the densities of the steady state populations.

5. Numerical simulations

In this section, we perform numerical simulations for our four dimensional mathematical model using Matlab 2016a to validate and justify all of our analytical findings achieved in the Sections 3.2, 3.3 and 4. These numerical findings help us interpreting the dynamical shifts of our system cell populations in presence of MDT and more specifically, the procedure of infection of recovered Schwann cells as a resultant of gradually waning drug dose efficiency. Separate simulations have been performed for PB and MB cases considering different

Table 1
List of parameter values used in numerical simulations for system (1).

Parameter	Parameter definition	Assigned value (Unit)	Range
Π	Production rate of healthy Schwann cells	35 (cells day^{-1})	20–50
β	Contact rate of *M. leprae* and healthy cells	0.0022 (mm^3 day^{-1})	0.0012–0.0058
α	Recovery rate of infected cells	0.0001 (mm^3 day^{-1})	0.00008–0.0002
λ	Infection rate due to fading effect of MDT	0.00042 (mm^3 day^{-1})	0.0002–0.00045
d	Natural death rate of healthy Schwann cell	0.004 (day^{-1})	0.0015–0.006
d_i	Natural death rate of infected Schwann cell	0.0036 (day^{-1})	0.0001–0.0046
η	Drug efficacy rate of MDT	0.026	–
r	Growth rate of *M. leprae* bacteria	0.1 (day^{-1})	–
K	Carrying capacity of the bacteria	500 (mm^{-3})	200–700
d_b	Rate at which *M. leprae* is killed by MDT	0.0022 (day^{-1})	0.0014–0.003
e	Proportionality constant	1.1	–
θ	Rate of flushing out of the drug MDT	0.00012 (μM day^{-1})	0.0001–0.0002

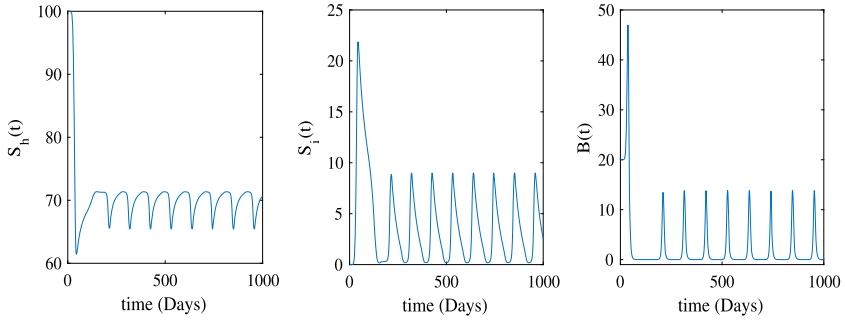

Fig. 2. Dynamical nature of the trajectories the healthy Schwann cells ($S_H(t)$), infected Schwann cells ($S_I(t)$), *M. leprae* bacteria ($B(t)$) of the system without drugs at the endemic state E^* for $R_0 > 1$. The initial values of the system populations are considered as: $S_H(0) = 100$, $S_I(0) = 5$, $B(0) = 20$ and values of all the other parameters are chosen from Table 1.

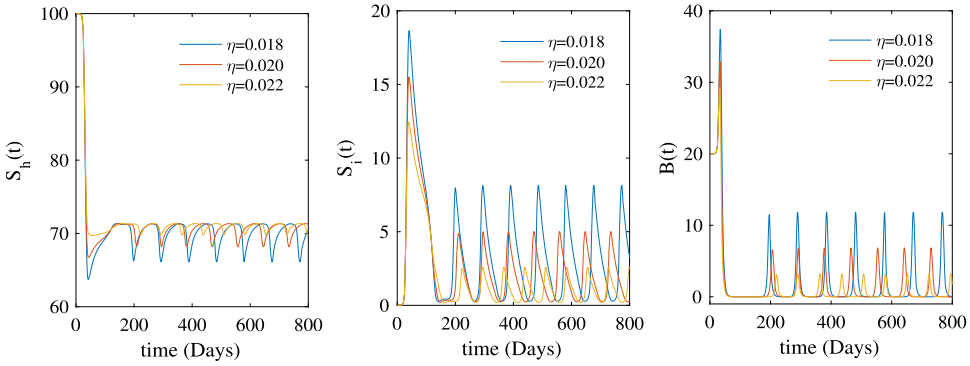

Fig. 3. Comparison of the oscillatory solutions of the healthy Schwann cells ($S_H(t)$), infected Schwann cells ($S_I(t)$), *M. leprae* bacteria ($B(t)$) of system (1) for different values of drug efficacy rate η at the steady state when $R_0 > 1$. Trajectories coloured in blue, red and brown indicate the densities of the system population for the values of $\eta = 0.018$, $\eta = 0.02$ and $\eta = 0.022$. Values of rest of the parameters used in the simulation of this figure are taken from Table 1.

values of infection rates depending on bacterial index (BI) and drug efficacy rates. To carry this out, we use a set of parameters provided in Table 1. Some of the values of these parameters for system (1) are assumed and other values are either obtained from several literatures or estimated from different elemental sources (Ghosh et al., 2021, 2022; Fischer, 2017; Talhari et al., 2015). For the purpose of numerical simulations, we have used the explicit forms as $f(X) = \frac{X}{1+X}$ and $g(X) = \frac{1}{1+X}$. We choose the initial values in number dependent according to the cardinal rule of scientific hypothesis.

In Fig. 2, we have demonstrated the behaviour of the trajectories of the system without drugs for $R_0 > 1$ at the endemic state E^*. It is evident that in this scenario, system cell populations exhibits periodic oscillatory solutions i.e. the densities of healthy Schwann cells ($S_H(t)$), infected Schwann cells ($S_I(t)$) and *M. leprae* bacteria ($B(t)$) fluctuate rapidly in the neighbourhood of E^* in the absence of drug. Biologically, it clearly justifies the essence of incorporating MDT therapy into the system for the densities of the system populations to arrive in a stable state.

Next, in Fig. 3, solution trajectories of the populations of system (1) the endemic state E^* have been described for three different values of η i.e. for the values of $\eta = 0.018, 0.02, 0.022$. Our findings suggests that amplitude of the fluctuation in the densities of S_H cells, S_I cells and *M. leprae* bacteria B decreases as η is increased from the value 0.018. This specific pattern indicates that the system populations tends to a stable concentration gradually with the increasing of the value of the drug efficacy rate η of MDT.

In Fig. 4, bifurcation diagrams of the populations of system (1) with respect to the efficacy rate η are depicted at a neighbourhood of the endemic equilibrium E^*. For the value of $\eta < 0.024$, periodic oscillatory solutions are observed but as the value of η crosses the critical value $\eta = \eta^* = 0.024$, system becomes stable. Thus, it clearly indicates that the efficacy rate of MDT, η plays a crucial role in leprosy pathogenesis as the whole dynamical shifting of the behaviour of the trajectories of the system cell populations depends primarily on this parameter. Biologically, this reflects that MDT therapy with an efficacy rate η greater than the threshold value $\eta = \eta^*$ is strictly recommended

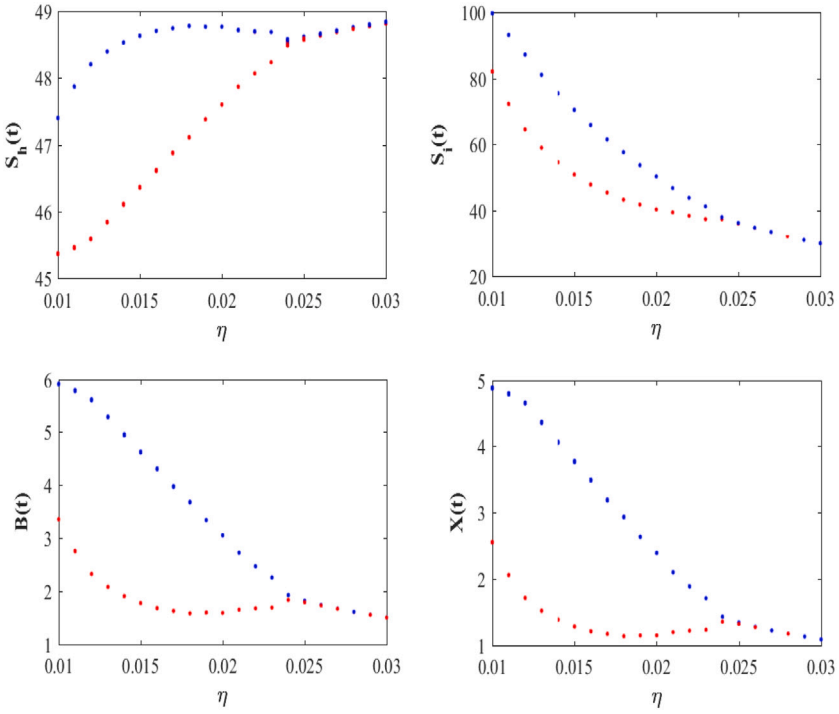

Fig. 4. Demonstration of bifurcation diagrams and oscillation of the model populations for system (1) plotted as a function of drug efficacy rate η for $R_0 > 1$. Here, steady state values of all the populations are plotted together with the minimum/maximum of the periodic solutions when it exists. We choose the values of the parameters as given in Table 1. Unstable and stable zones are clearly displayed by the dotted vertical line drawn at the critical value $\eta = \eta^* = 0.024$.

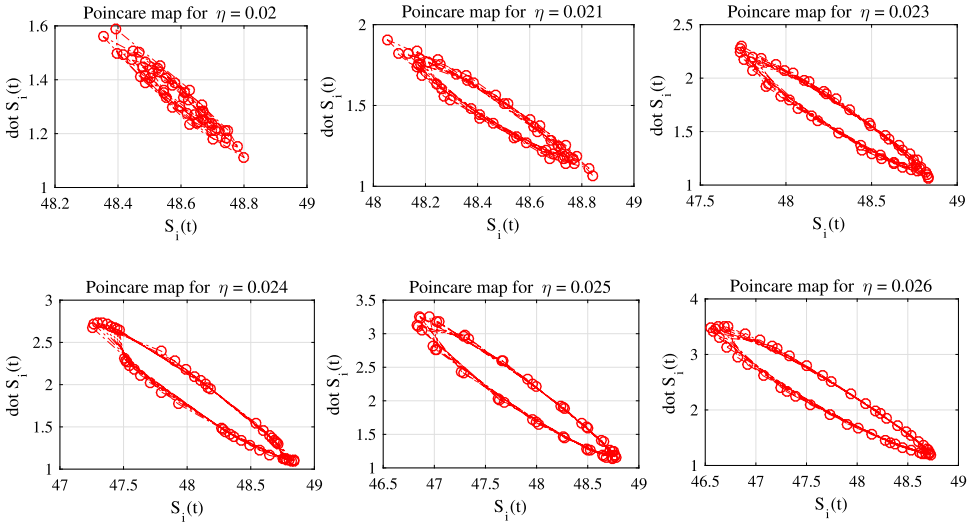

Fig. 5. Poincare section for the set of parameter values for system (1). Here, the investigation is performed for six different values of efficacy rate η to achieve the six subfigures. The values of parameters are chosen as $\Pi = 50$ cells day^{-1}, $\beta = 0.00014$ mm^3 day^{-1} and all the other parameters are taken from Table 1.

to reduce the disease dissemination process effectively into the human body.

In Fig. 5, we have demonstrated the Poincare section for the parameter values of system (1) represented in Table 1. Here, we have actually plotted $\dot{S}_i(t)$ vs $S_i(t)$ using six different values of η. The discrete dynamical behaviour of our continuous system (1) through the intersection of periodic orbits in the state space is investigated and represented here to establish a permissible range of drug efficacy η for which the system remains stable. This figure describes that the points assemble together to form a definite pattern occupying a subset of the phase space. The values of $\dot{S}_i(t)$ ranges over nearly ≈ 1 to 3.56 for all the subfigures but we can see that this specific pattern is not deviated or more particularly, for the values of $\eta = 0.024, 0.025, 0.026$, it does not lose the shape as the values of $S_i(t)$ is increased. This dynamical nature of system (1) precisely forms the origination of an attractor such that the system trajectories intersect the plane in this pattern. This attractor is a limit cycle and hence, we can conclude that the system is stable for this specific ranges of values of η. Also, from this figure, our findings confirm the global asymptotical stability of system (1) as we have opted for Poincare section method here in exhibiting this phenomenon instead of extensive and tedious analytical calculations.

Next, in Fig. 6, we have plotted time evolution of the sum of all four Lyapunov's exponents of the model populations for system (1) for different values of η and the corresponding dynamics of Lyapunov's exponents are described. To indicate the PB types of cases, the value of β is chosen considerably low i.e.$\beta = 0.0032$ mm^3 day^{-1}. The values

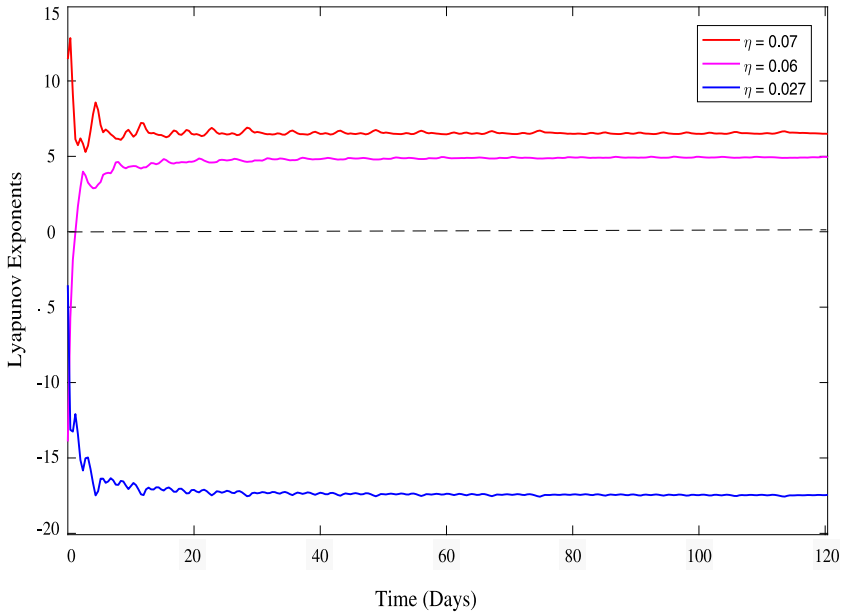

Fig. 6. Plot of the sum of all the Lyapunov's exponents of the model cell populations for system (1) for Paucibacillary (PB) types of infection. Values of the parameters are taken $\beta = 0.0032$ mm^3 day^{-1} and $K = 420$ mm^{-3} and the values of the other parameters are chosen from Table 1. Trajectories coloured in blue, pink and red indicate the dynamics of the sum of the exponents of S_H cells, S_I cells, bacteria $B(t)$ and MDT concentration $X(t)$ with time for the values of $\eta = 0.027$, $\eta = 0.06$ and $\eta = 0.07$ respectively.

of drug-efficacy rate η are chosen as $\eta = 0.027, 0.06$ and 0.07 and all the other parameter values are chosen here according to the values given in Table 1. Investigating the Lyapunov's exponents for our system enables us to detect the presence of chaos and quantify the stability or instability of the system. Fig. 6 actually determines the system's sensitivity to initial conditions and more precisely, measures the robustness of the densities of the system populations: S_{h_0}, S_{i_0}, B_0 and X_0 at the time $t = 0$. Moreover, positivity of the sum of Lyapunov exponents means that the system is sensitive to the initial values and possesses chaotic nature. The obtained dynamics of Lyapunov's exponents explains that for $\eta = 0.027$, the sum of the exponents remains negative suggesting that system (1) remains stable in this case. This finding also supports the results achieved in Fig. 4. Also, for higher values of efficacy rate i.e. for $\eta = 0.06, 0.07$, system exhibits chaotic behaviour and ultimately, becomes unstable again which is validated by the positive values of sum of Lyapunov's exponents of all the system populations. Specifically, it suggests us that applying MDT for a prolonged period of time i.e. from 6 months to 12 months in PB cases with a very high efficacy rate (i.e. for $\eta > 0.059$) on a leprosy affected person, does not actually exhibit any fruitful result (Narang et al., 2022). Rather, it induces substantial drug resistance (Sansarricq, 2004) and severe adverse drug effects (Deps et al., 2007; Kaluarachchi et al., 2001) into the human body. This indicates a treatment tenure of at least 120 days for PB cases which also supports the WHO recommended PB multidrug therapy regimen completely (World Health Organization, 1998).

Similarly, in Fig. 7, time evolution of the sum of all the Lyapunov's exponents of our system cell populations are demonstrated for the values of $\eta = 0.055, 0.06$ and 0.07 for 300 days. To simulate this figure, value of β is considered as $\beta = 0.0071$ to specifically indicate the infection rate of multibacillary (MB) types of leprosy patients. Simulation shows that our system populations starts getting stabilized after 300 days of treatment with safe and effective efficacy zone of $\eta \in (0.025, 0.059)$ which is also recognized by the WHO mentioned guidelines for multibacillary leprosy patients.

Fig. 8 investigates and presents the sensitivity of the level of treatment i.e. the drug efficacy rate (η) which we incorporate in the system with time as the infection rate (β) increases. The values of β has been varied in the range 0.001–0.009 to simulate this figure. According to the sensitivity profile displayed in this figure, we can clearly see that

Table 2
Classification of the influence of MDT based on the values of η for system (1).

Range of values of η	Overall impact of MDT on a leprosy patient
$0 < \eta \leq 0.024$	Ineffective or mildly effective
$0.025 < \eta < 0.059$	Safe and strongly effective
$\eta \geq 0.06$	Unsafe

η is highly sensitive to the infection rate β which regulates the overall progression of infection into a leprosy patient.

Finally, the combined impact of η and λ on the basic reproduction number R_0 and also the impact of η and β on R_0 has been displayed in the subfigure (a) and subfigure (b) respectively in Fig. 9. In subfigure (a), we have demonstrated the contour plot of η, λ and R_0 in the three dimensional space where both the values of η and λ are varied over the interval $(0, 1)$. The plane denoted by $R_0 = 1$ plays a decisive role here as it intersects the other two planes. This intersection particularly contributes to present the coupled threshold values of level of treatment where η plays a determining role for the control of the disease progression. In the contour plot denoted by subfigure (b), the intersection of the plane $R_0 = 1$ provides us a decisive criteria for the feasibility of the endemic state E^* and its dependency on the two most significant parameters η and β for finding an effective yet safe drug dose regimen for leprosy.

In view of the above numerical simulations and the analytical results obtained in the previous sections, we now present the following Table 2 which describes the dynamical behaviour of the system and overall impact of the multidrug therapy for different values of efficacy rate η into a leprosy affected person.

6. Discussion and conclusion

Leprosy is a chronic disorder of the peripheral nervous system which continues to remain as one of the most neglected tropical diseases in the last few decades. Clinical researchers and biologists have done many experiments in the past years to decode the disease dynamics of leprosy. Still, the fundamental issues involving the drug-effectiveness of MDT therapy, drug overdose situation, proper length or duration

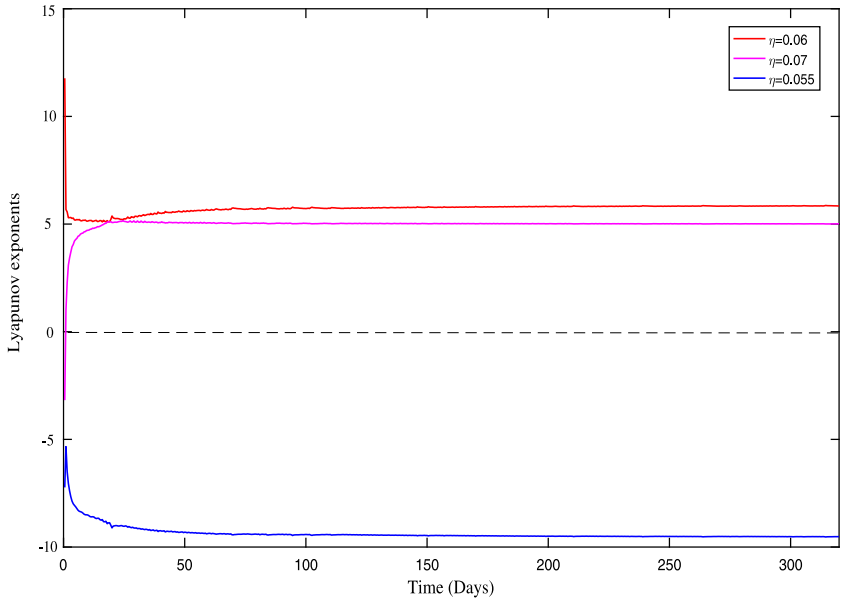

Fig. 7. Plot of the sum of all the Lyapunov's exponents of the model cell populations for system (1) for Multibacillary (MB) types of infection. Values of the parameters are taken $\beta = 0.0071$ mm^3 day^{-1} and $K = 480$ mm^{-3} and the values of the other parameters are chosen from Table 1. Trajectories coloured in blue, pink and red indicate the dynamics of the sum of the exponents of S_H cells, S_I cells, bacteria $B(t)$ and MDT concentration $X(t)$ with time for the values of $\eta = 0.055$, $\eta = 0.07$ and $\eta = 0.06$ respectively.

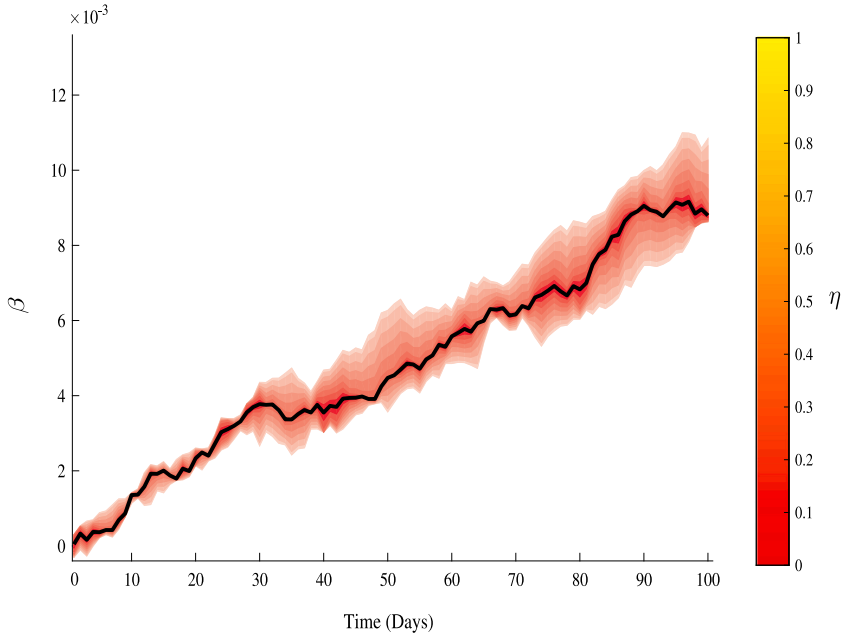

Fig. 8. Analysis of the sensitivity of the drug efficacy rate (η) with time as the infection rate (β) increases for system (1) for 100 days of treatment. As the colour becomes darker from light, the figure indicates a higher sensitivity profile. All the parameter values are chosen from Table 1 to simulate this figure.

of treatment, adverse therapeutic effects and re-emergence of the infection (Sales et al., 2013; Gelber and Grosset, 2012; Penna, 2014) into the human body are hardly investigated and analysed from a mathematical point of view. To fill these gaps, we have presented a four dimensional nonlinear ODE based mathematical model describing the infection of healthy Schwann cells and recovery of the infected cells of the peripheral nervous system through multidrug therapy.

We have obtained mathematical constraint about the existence of the positive endemic equilibrium E^* in Lemma 3.1 in Section 3.2 and the local asymptotical stability conditions of system (1) at E^* in Theorem 3.4 by using the well-known Routh–Hurwitz criterion. We have also derived the basic reproduction number R_0 for system (1). When R_0 greater than unity, the disease-free equilibrium E_0 exists and becomes unstable. Here, E^* emerges for $R_0 > 1$ which suggests that the disease starts invading the healthy cell population in this scenario. On the other hand, for $R_0 < 1$, the disease leprosy is eliminated and this clearly indicates occurrence of a transcritical bifurcation at the critical value $R_0 = 1$. The necessarily required transversality condition for the occurrence of Hopf-bifurcation is established by Theorem 4.1 in Section 4 which indicates that system (1) behaves in a stable manner as η crosses the threshold value η^*. This behavioural change in the pattern of the solutions of the system is observed due to the downregulating and reprogramming effect of healthy adult cells within the body of a leprosy affected person as demonstrated by Masaki et al. (2013).

During the investigation of system (1), we have used some parameters for exhibiting numerical examples and to make our model

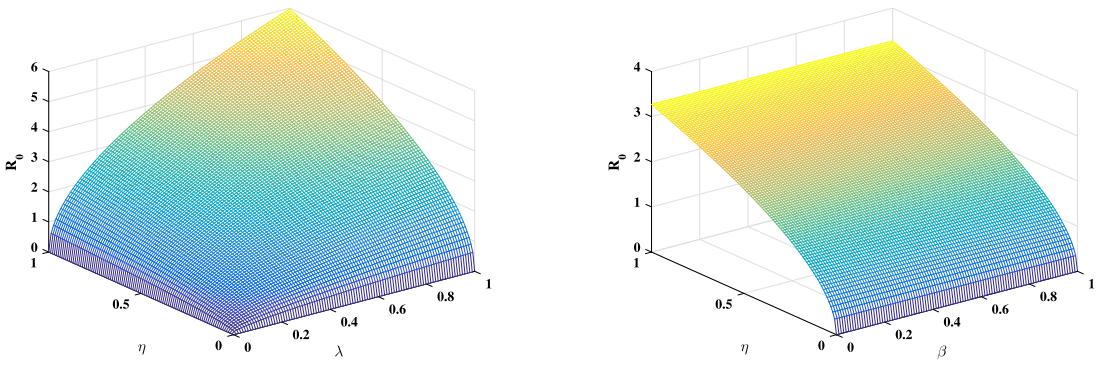

(a) contour plot of η, λ and R_0 (b) contour plot of η, β and R_0

Fig. 9. Three dimensional contour plots of different pairs of parameters with the basic reproduction number R_0 for system (1). Values of rest of the parameters used here are chosen from Table 1.

biologically reasonable which are hypothetically assumed due to the unavailability of sufficient real clinical data. If proper ranges of values of these parameters were available, it would be possible to frame the drug dose regimens more realistically. Our proposed treatment design should necessarily be used for future pharmaceutical trials after considering the results from proper clinical experiments. Also, it is important to note that the actual mode of mechanism of MDT on infected Schwann cells are still very complicated and not completely explored by the scientists. Due to this reason, we have chosen $f(X)$ and $g(X)$ in the general functional form rather using any explicit mathematical expression. Any strictly monotonic increasing and decreasing real-valued function with $f(0) = 0$, $g(0) = 1$, $\sup f(X) = 1$ and $\inf g(X) = 0$ defined on $\mathbb{R}$ would perfectly fit into our model as $f(X)$ and $g(X)$ respectively so that any futuristic work on leprosy considering our system would surely be benefited. In addition, future works on leprosy can also be performed in this direction by constructing different mathematical models for PB and MB types of infections to look into the finer details of the leprosy dynamics.

We have also compared our analytical findings with the numerical results obtained in Section 5. The numerical interpretations in Figs. 3–6 completely suggest us that varying the drug efficacy rate of all the three components of MDT within the fixed range 0.025–0.059 for approximately 120 days in PB cases and 300 days in MB cases helps the system getting stabilized and thus, the dissemination of leprosy to different human organs can evidently be controlled. Impact of MDT has explored two simultaneously occurring phenomenon i.e. the spontaneous recovery of the infected cells S_i and the re-infection of the recovered cells due to the waning effect of MDT which predicts that the drug efficacy rate η of MDT is the most influential parameter for system (1) monitoring the overall stability situation and dynamical shift of the system. For very low efficacy rate, weak bactericidal activity of MDT against *M. leprae* is noted. Due to this, for $\eta \leq \eta^* = 0.024$, oscillatory periodic solutions of system (1) are noticed which indicates that MDT in this low efficacy zone is ineffective and any notable improvement in the reduction of the bacterial load are not observed (Shepard, 1981; Prasad and Kaviarasan, 2010). This findings is also supported by the recent clinical studies (Penna et al., 2012, 2017) where based on the randomized and controlled clinical trial on 613 newly diagonized untreated leprosy patients in China, India and Bangladesh, the authors have confirmed that an uniform treatment method called uniform multidrug therapy (U-MDT) can be an acceptable option for future treatment of leprosy worldwide especially in the endemic countries. Moreover, from the findings of Figs. 6, 8 and Table 2, we can interpret that for the range of values of $\eta > 0.06$, solutions of system (1) becomes chaotic and ultimately unstable. Hence, incorporating an abruptly higher drug dose is unsafe for the leprosy patients and would eventually have a negative effect on the human body because it induces drug resistance and severe adverse drug effects such as irreversible nerve damages, blindness etc. (Guragain et al., 2017; Sansarricq, 2004).

Considering the Ridley–Jopling classification of leprosy (Ridley and Jopling, 1966), we can see that due to higher values of intrinsic growth rate (r) and carrying capacity (K) of *M. leprae*, higher range of values of η in between 0.052–0.059 should necessarily be used as an effective treatment method for lepromatous leprosy cases (LL). For PB cases (especially in tuberculoid TT), our analytical and numerical findings from Figs. 5, 6 and 8 suggests that a lesser efficacy rate of varying η within the range 0.025–0.04 for nearly 120 days will be more beneficial due to the smear-negative property and low bacterial index with BI < 2 (skin lesions ≤ 5). Clinical studies validate this finding also as the outcomes of Prasad and Kaviarasan (2010) suggests that PB patients are mostly found to be lepromin-positive and after completion of therapy, the residual organisms into the human body will be tackled by the host immune response.

Framing a shorter period of effective treatment policy is of major importance always to avoid relapse and irregularities in treatment (Gelber et al., 2004; Girdhar et al., 2000). Considering the WHO recommended classification, there are two major types of leprosy depending on the count of bacterial load in the skin smears and these are as follows : Paucibacillary leprosy (PB) for bacterial index BI < 2 and Multibacillary leprosy (MB) for BI $\geq$ 2. The reduced multidrug therapy regimen recommended by WHO for leprosy is scheduled as 6 months in PB cases and 6 - 12 months in MB cases (World Health Organization, 1998; Renault and Ernst, 2015; Rodrigues and Lockwood, 2011). During the numerical simulation portion, specifically in Fig. 6, we have chosen the value of infection rate $\beta = 0.0032$ considerably low to indicate actually the infection of PB types of leprosy patients. This produces the result that the system starts getting stabilized after 120 days i.e. at least 120 days (or 4 months) of treatment with maintaining the efficacy range $\eta \in (0.025, 0.059)$ is recommended for PB cases. For the infection of MB types of patients, bacterial load is much higher as BI $\geq$ 2 and hence, $\beta = 0.0071$ is chosen to simulate Fig. 7. In this case, our outcomes in Figs. 4, 7 suggest that drug efficacy rate η cannot be increased more than 0.059 as the cell concentrations of our system becomes unstable. This evidently indicates the essence of applying a flexible version of MDT therapy with η in the safe and effective zone i.e. $\eta \in (0.025, 0.059)$ but necessarily for a longer treatment period of nearly 300 days [10 months] for MB cases as demonstrated in Fig. 7. Thus, our suggested treatment policy is clearly effective, avoids the concerns of drug resistance, adverse drug effects and supports the WHO recommended treatment regime for both PB and MB types of leprosy

patients but modified as an effect of the crucial interplay of the most significant parameter drug efficacy rate η of MDT.

After 12 months, presence of viable load of bacilli after treatment with MDT are observed in some specific cases for patients with high bacillary load (Shetty et al., 2003; Narang et al., 2022; Kar et al., 2004; Gupta et al., 2005). Hence, strict long-term followup is needed and the overall health situations of every leprosy patient should be monitored very carefully after RFT (release for treatment). Indeed, if required, for the PB patients and especially, for the MB patients with high initial BI (Prasad and Kaviarasan, 2010), the pattern of sensitivity profile of η vs. β demonstrated in Fig. 8 and Table 2 suggests that treatment can be continued after the recommended period within the prescribed drug efficacy zone for some cases considering different status of the disease.

In our current research work, we have discussed a four dimensional mathematical model which successfully captures some basic and intriguing features of the disease dissemination process and therapeutic approaches for leprosy. Our proposed treatment policy with a flexible version of MDT with the prescribed zone of drug efficacy rate and treatment tenures for both paucibacillary and multibacillary types of patients is much safer, effective and can really be a potential candidate for future clinical trials and for the pharmacists aiming to develop a realistic and accurate treatment regime.

Financial disclosure

This research work is supported by the W.B. Government State Fellowship, Government of West Bengal, India. The research work is also supported by DST-FIST, Department of Mathematics, Jadavpur University, Kolkata - 700032, India.

CRediT authorship contribution statement

Salil Ghosh: Conceptualization, Data curation, Writing – original draft, Formal analysis, Contributed analysis tools, Analysed and interpreted the results. **Shubhankar Saha:** Performed the computer simulations. **Priti Kumar Roy:** Overall supervised the whole manuscript.

Declaration of competing interest

The authors declare that they have no known competing financial interests or personal relationships that could have appeared to influence the work reported in this paper.

References

Birkhoff, G., Rota, G.C., 1978. Ordinary Differential Equations (Vol. 4). Wiley, New York.
Britton, W.J., 1998. The management of leprosy reversal reactions. Lepr. Rev. 69 (3), 225–234.
Cao, X., Saha, S., Roy, P.K., 2019. A statistical inference in an epidemic model with combinational drug treatment: HIV as a case study. Results Appl. Math. 3, 100066.
Deps, P.D., Nasser, S., Guerra, P., Simon, M., Birshner, R.D.C., Rodrigues, L.C., 2007. Adverse effects from multi-drug therapy in leprosy: A Brazilian study. Lepr. Rev. 78 (3), 216–222.
Fischer, M., 2017. Leprosy–an overview of clinical features, diagnosis, and treatment. JDDG: J. Der Deutschen Dermatol. Gesellschaft 15 (8), 801–827.
Gelber, R.H., Balagon, M.V.F., Cellona, R.V., 2004. The relapse rate in MB leprosy patients treated with 2-years of WHO-MDT is not Low1. Int. J. Lepr. Other Mycobact. Dis. 72 (4), 493.
Gelber, R.H., Grosset, J., 2012. The chemotherapy of leprosy: An interpretive history. Lepr. Rev. 83 (3), 221–240.
Ghosh, S., Chatterjee, A.N., Roy, P.K., Grigorenko, N., Khailov, E., Grigorieva, E., 2021. Mathematical modeling and control of the cell dynamics in leprosy. Comput. Math. Model. 32 (1), 52–74.
Ghosh, S., Rana, S., Roy, P.K., 2022. Leprosy: Considering the effects on density-dependent growth of mycobacterium leprae. Differ. Equ. Dyn. Syst. 1–15.
Girdhar, B.K., Girdhar, A.N.I.T.A., Kumar, A.N.I.L., 2000. Relapses in multibacillary leprosy patients: Effect of length of therapy. Lepr. Rev. 71 (2), 144–153.
Gupta, U.D., Katoch, K., Singh, H.B., Natrajan, M., Katoch, V.M., 2005. Persister studies in leprosy patients after multi-drug treatment. Int. J. Lepr. Other Mycobact. Dis. 73 (2), 100.
Guragain, S., Upadhayay, N., Bhattarai, B.M., 2017. Adverse reactions in leprosy patients who underwent dapsone multidrug therapy: A retrospective study. Clin. Pharmacol.: Adv. Appl. 9 (73).
Heffernan, J.M., Smith, R.J., Wahl, L.M., 2005. Perspectives on the basic reproductive ratio. J. R. Soc. Interface 2 (4), 281–293.
Ikeda, Y., Takeuchi, Y., Martin, F., Cosset, F.L., Mitrophanous, K., Collins, M., 2003. Continuous high-titer HIV-1 vector production. Nature Biotechnol. 21 (5), 569–572.
Kaluarachchi, S.I., Fernandopulle, B.M., Gunawardane, B.P., 2001. Hepatic and haematological adverse reactions associated with the use of multidrug therapy in leprosy–A five year retrospective study. Indian J. Lepr. 73 (2), 121–129.
Kar, B.R., Belliappa, P.R., Ebenezer, G., Job, C.K., 2004. Single lesion borderline lepromatous leprosy. Int. J. Lepr. Other Mycobact. Dis. 72, 45–47.
Krasnosel'skii, M.A., 1968. The Operator of Translation Along the Trajectories of Differential Equations (Vol. 19). Amer Mathematical Society.
Kroger, A., Pannikar, V., Htoon, M.T., Jamesh, A., Katoch, K., Krishnamurthy, P., Ramalingam, K., Jianping, S., Jadhav, V., Gupte, M.D., Manickam, P., 2008. International open trial of uniform multi-drug therapy regimen for 6 months for all types of leprosy patients: Rationale, design and preliminary results. Trop. Med. Int. Health 13 (5), 594–602.
Lockwood, D.N., Suneetha, S., 2005. Leprosy: Too complex a disease for a simple elimination paradigm. Bull. World Health Org. 83, 230–235.
Masaki, T., Qu, J., Cholewa-Waclaw, J., Burr, K., Raaum, R., Rambukkana, A., 2013. Reprogramming adult schwann cells to stem cell-like cells by leprosy bacilli promotes dissemination of infection. Cell 152 (1–2), 51–67.
Meima, A., Smith, W.C.S., Van Oortmarssen, G.J., Richardus, J.H., Habbema, J.D.F., 2004. The future incidence of leprosy: A scenario analysis. Bull. World Health Org. 82, 373–380.
Narang, T., Kamat, D., Thakur, V., Lavania, M., Singh, I., Ahuja, M., Dogra, S., 2022. Equal rates of drug resistance in leprosy cases with relapse and recurrent/chronic type 2 reaction: Time to revise the guidelines for drug-resistance testing in leprosy? Clin. Exp. Dermatol. 47 (2), 297–302.
Ng, V., Zanazzi, G., Timpl, R., Talts, J.F., Salzer, J.L., Brennan, P.J., Rambukkana, A., 2000. Role of the cell wall phenolic glycolipid-1 in the peripheral nerve predilection of Mycobacterium leprae. Cell 103 (3), 511–524.
Parkash, O., 2009. Classification of leprosy into multibacillary and paucibacillary groups: An analysis. FEMS Immunol. Med. Microbiol. 55 (1), 1–5.
Penna, M.L.F., 2014. Considerations in the design of clinical trials for multibacillary leprosy treatment. Clin. Invest. 4 (1), 77–86.
Penna, G.O., Bührer-Sékula, S., Kerr, L.R.S., Stefani, M.M.D.A., Rodrigues, L.C., de Araújo, M.G., Ramos, A.M.C., de Andrade, A.R.C., Costa, M.B., Rosa, P.S., Gonçalves, H.D.S., 2017. Uniform multidrug therapy for leprosy patients in Brazil (u-MDT/CT-BR): Results of an open label, randomized and controlled clinical trial, among multibacillary patients. PLoS Negl. Trop. Dis. 11 (7), e0005725.
Penna, M.L.F., Buhrer-Sekula, S., Pontes, M.A.D.A., Cruz, R., Gonçalves, H.D.S., Penna, G.O., 2014. Results from the clinical trial of uniform multidrug therapy for leprosy patients in Brazil (u-MDT/CT-BR): Decrease in bacteriological index. Lepr. Rev. 85 (4), 262–266.
Penna, G.O., Pontes, M.A.D.A., Cruz, R., Gonçalves, H.D.S., Penna, M.L.F., Bührer-Sékula, S., 2012. A clinical trial for uniform multidrug therapy for leprosy patients in Brazil: Rationale and design. Memórias Do Inst. Oswaldo Cruz 107, 22–27.
Prasad, P.V.S., Kaviarasan, P.K., 2010. Leprosy therapy, past and present: Can we hope to eliminate it? Indian J. Dermatol. 55 (4), 316.
Rambukkana, A., 2001. Molecular basis for the peripheral nerve predilection of Mycobacterium leprae. Curr. Opin. Microbiol. 4 (1), 21–27.
Rambukkana, A., 2010. Usage of signaling in neurodegeneration and regeneration of peripheral nerves by leprosy bacteria. Progress Neurobiol. 91 (2), 102–107.
Renault, C.A., Ernst, J.D., 2015. Mycobacterium leprae (leprosy). In: Mandell, Douglas, and Bennett's Principles and Practice of Infectious Diseases. WB Saunders, pp. 2819–2831.
Ridley, D.S., Jopling, W.H., 1966. Classification of leprosy according to immunity. Int. J. Lepr. Other Mycobact. Dis. 34, 255–273.
Rodrigues, L.C., Lockwood, D.N., 2011. Leprosy now: Epidemiology, progress, challenges, and research gaps. Lancet Infect. Dis. 11 (6), 464–470.
Saha, S., Roy, P.K., SMITH?, R.O.B.E.R.T., 2018. Modeling monocyte-derived dendritic cells as a therapeutic vaccine against HIV. J. Biol. Systems 26 (04), 579–601.
Sales, A.M., Campos, D.P., Hacker, M.A., da Costa Nery, J.A., Düppre, N.C., Rangel, E., Sarno, E.N., Penna, M.L.F., 2013. Progression of leprosy disability after discharge: Is multidrug therapy enough? Trop. Med. Int. Health 18 (9), 1145–1153.
Sansarricq, H., 2004. Multidrug Therapy Against Leprosy: Development and Implementation over the Past 25 Years (No. WHO/CDS/CPE/CEE/2004.46). World Health Organization.
Scollard, D.M., Adams, L.B., Gillis, T.P., Krahenbuhl, J.L., Truman, R.W., Williams, D.L., 2006. The continuing challenges of leprosy. Clin. Microbiol. Rev. 19 (2), 338–381.
Shepard, C.C., 1981. A brief review of experiences with short-term clinical trials monitored by mouse-foot-pad inoculation. Lepr. Rev. 52 (4), 299–308.
Shetty, V.P., Wakade, A.V., Ghate, S., Pai, V.V., Ganapati, R., Antia, N.H., 2003. Viability and drug susceptibility testing of M. leprae using mouse footpad in 37 relapse cases of leprosy. Int. J. Lepr. Other Mycobact. Dis. 71 (3), 210–217.
Smith, R.J., Wahl, L.M., 2005. Drug resistance in an immunological model of HIV-1 infection with impulsive drug effects. Bull. Math. Biol. 67 (4), 783–813.

Talhari, C., Talhari, S., Penna, G.O., 2015. Clinical aspects of leprosy. Clin. Dermatol. 33 (1), 26–37.
Walker, S.L., Lockwood, D.N.J., 2006. The clinical and immunological features of leprosy. Br. Med. Bull. 77 (1), 103–121.
White, C., Franco-Paredes, C., 2015. Leprosy in the 21st century. Clin. Microbiol. Rev. 28 (1), 80–94.
Wilder-Smith, E.P., Van Brakel, W.H., 2008. Nerve damage in leprosy and its management. Nat. Clin. Pract. Neurol. 4 (12), 656–663.
WJ, B., 2004. Lockwood DN. Leprosy. Lancet 363, 1209–1219.
World Health Organization, 1998. WHO Expert Committee on Leprosy: Seventh Report. World Health Organization.